SCIENTIFIC BRIEFING

HP TODAY

Ground-based thermal imagery as a simple, practical tool for mapping saturated area connectivity and dynamics

Laurent Pfister,[1]*
Jeffrey J. McDonnell,[2,3]
Christophe Hissler[1] and
Lucien Hoffmann[1]

[1] *Centre de Recherche Public—Gabriel Lippmann, Department Environnement et Agro-biotechnologies, 41 rue du Brill, L-4422 Belvaux, Luxembourg*
[2] *Department of Forest Engineering, Oregon State University, 015 Peavy Hall, Corvallis, OR 97331-5706, USA*
[3] *School of Geosciences, University of Aberdeen, Aberdeen AB243UF, Scotland, UK*

*Correspondence to:
Laurent Pfister, Department Environnement et Agro-biotechnologies, Centre de Recherche Public—Gabriel Lippmann, 41 rue du Brill, L-4422 Belvaux, Luxembourg.
E-mail: pfister@lippmann.lu*

Abstract

The hillslope-riparian-stream system is a key functional unit of catchments, yet very difficult to measure and monitor due to its tremendous complexity and high spatio-temporal variability. Here, we present a simple and practical tool for imaging directly these hillslope-riparian-area connections. We used a FLIR b50 infrared camera to produce thermal images at the scale of 140×140 pixels over the spectral range 7·5–13 μm. Our IR imaging technique is sensitive to the upper 0·1 mm of the water column. Images were obtained from a constant position on the right bank of the Weierbach catchment in Luxembourg, at an incidence angle of approximately 45° over a 5-week period. The study site measured 5×3 m. Our results show that ground-based IR imagery can discriminate between areas with snow cover, snow melt, soil seepage, and stream water. More importantly, it can detect when and where variably saturated areas are active and when connectivity exists between the hillslope–riparian–stream system. Our proof of concept suggests that this is a simple, inexpensive technology for sequential mapping and characterisation of surface saturated areas and a useful complement to conventional tracer techniques. Copyright © 2010 John Wiley & Sons, Ltd.

Key Words thermal infrared; saturated area connectivity; variable active area; variable contributing area

Introduction

Surface water connections between the hillslope–riparian–stream (HRS) system are complex and highly variable in time and space (O'Loughlin, 1981; Jencso *et al.*, 2009). While still poorly understood, they are known to have a first-order control on run-off generation and resulting streamflow response (Bonell, 1993), DOC and N transformations (Cirmo and McDonnell, 1997), as well as the fate and transport of dissolved constituents to the stream (Gburek *et al.*, 2002).

The measurement and documentation of HRS connectivity is a major impediment to better process understanding. The mapping of the HRS connection was the subject of active field work many decades ago (Dunne *et al.*, 1975), but stalled in recent years. The foundational work during the First International Hydrological Decade relied on 'squishy boot' mapping and delineation of surface-saturated areas around the stream channel (Dunne and Black, 1970). While these techniques became more sophisticated with later incorporation of topography-soil-vegetation analysis (O'Loughlin, 1981), remote sensing (Verhoest *et al.*, 1998; Matgen *et al.*, 2006) and GIS-based approaches (Zollweg *et al.*, 1997), much of the work recently has been focused on incorporating saturated area dynamics into models (Frankenberger *et al.*, 1999; Kuo *et al.*, 1999; Ogden and Watts, 2000). More recently, Jencso *et al.* (2009) have transferred reach- and plot-scale understanding to the catchment scale via distributed well transects.

While new progress is being made in quantifying and describing HRS dynamics, direct measurement of these linkages is still a major problem and limitation. One approach to quantifying HRS connectivity not yet fully exploited is thermal imagery. Point measurements of stream temperature have been used for decades in water quality studies (e.g. Smith, 1981; Webb and Walling, 1985, 1992; Webb and Nobilis, 1995; Gu *et al.*, 1998). More recently, distributed fibre optic point measurements of stream temperature have shown considerable promise as a proxy detecting groundwater-streamflow linkages (Selker *et al.*, 2006). Despite their recent contribution to the field (Roth *et al.*, 2010), distributed fibre optic measurements are restricted to the stream channel and the area immediately adjacent to the cable, with no measurement extension to the riparian or hillslope zone. At the other end of the measurement spectrum, airborne thermal infrared imaging has been used for large-scale wetness mapping (e.g. Roxburgh, 1985) and in agricultural and irrigation engineering applications (e.g. Anderson *et al.*, 2004). Especially in forested environments, airborne mapping suffers from little fidelity (and poor repeatability) for quantifying fine-scale HRS processes and connectivity dynamics. New approaches are sorely needed in between the point scale and airborne scale, particularly for forested headwater environments, where HRS linkages are most tightly coupled. Ground-based thermal imagery appears as a promising new avenue for investigating hydrological processes in the riparian zone at centimeter scale. Deitchman and Loheide (2009) have recently documented that heat can be used as a tracer for mapping the transition between saturated and unsaturated zones at the groundwater seepage face.

Here we present a new, simple thermal IR approach for imaging directly the HRS connection. Such portable hand-held thermal IR cameras are increasingly affordable and have recently been shown to be powerful tools for quantifying temperature variability on scales similar to those of interest in HRS research (Cardenas *et al.*, 2008). We present proof of concept for how thermal IR images can help quantify the spatial and temporal variability of streamflow generating processes occurring at the HRS interface. Specifically, we show the value of thermal IR for tracing riparian water sources, tracing surface water flowpaths and documenting HRS connectivity. In particular, we show how ponded rainfall and snowmelt, soil water and groundwater seepage can be distinguished with thermal IR imagery to ultimately infer surface water flowpaths, mixing areas and HRS connectivity.

Study Area

The study area for the thermal IR imaging experiments is the Weierbach experimental catchment in the Grand-duchy of Luxembourg (Europe), described in detail by Martínez-Carreras *et al*. (2010). The Weierbach is part of a network of 11 nested catchments located in the Attert

River basin. The Attert group of catchments has recently been used for various investigations on water source and flowpaths, including geochemical (Krein *et al.*, 2007; Martínez-Carreras *et al.*, 2010), isotope (Kies *et al.*, 2005) and biological (diatoms) tracers (Pfister *et al.*, 2009).

The Weierbach catchment covers an area of 0·45 km^2 and has steep slopes. Soils are shallow (10–70 cm) and consist of Haplic Cambisol (loamy, skeletic) and Stagnic Cambisol (loamy, skeletic) on plateaus and hillslopes, as well as Humic Fluvisol (loamy, skeletic) in the riparian areas. These soils cover a deep, permeable regolith of up to 10–25 m. The catchment is underlain by Devonian schists. Vegetation consists of mixed oak, beech, spruce, and Douglas fir forest stands. Annual average precipitation reaches 914 mm/year, of which approximately 470 mm/year form stream run-off (average values for the recording period July 2004–June 2008). Baseflow contributions are highest during winter and early spring and low during summer—reflecting the lack of a distinct riparian aquifer. Spring storm hydrograph separations based on silica and conductivity have shown small surface run-off influences on total flow in the Weierbach, in comparison to the much larger subsurface flow and transient groundwater from the schist regolith upslope (Krein *et al.*, 2007).

In this study, we focus on a 5 × 3 m site located some 25 m upstream of the Weierbach catchment outlet and streamgauge (Figure 1). We monitored stream water temperature via a WTW Tetracon 325 temperature probe. In the vicinity of the streamgauge, riparian groundwater level, and temperature were recorded every 15 min with a CTD-Diver pressure transducer probe. Rainfall and air temperature data for the site are from a Campbell Scientific meteorological station located approximately 2·5 km south of the Weierbach catchment. These measurements were used to describe the general meteorological conditions that had prevailed during the investigation phase in the area of interest.

Material and Methods

Thermal IR images of the hillslope, riparian zone, and stream channel (Figure 1) were taken with a portable FLIR b50 infrared camera. The thermal images were 140 × 140 pixels and covered a spectral range of 7·5–13 μm. The (claimed) temperature range of the camera is −20–120 °C, with a thermal sensitivity of approximately 0·09 at 25 °C.

The thermal IR imaging technique is sensitive to the upper 0·1 mm of the water column (Anderson and Wilson, 1984). Differences between radiant temperatures detected with the thermal IR camera and the in-stream thermometer were less than 1 °C. Emissivity was considered constant at 0·97 in all images because the main focus of image interpretation was the surface water temperature pattern. Air temperature and relative humidity data were
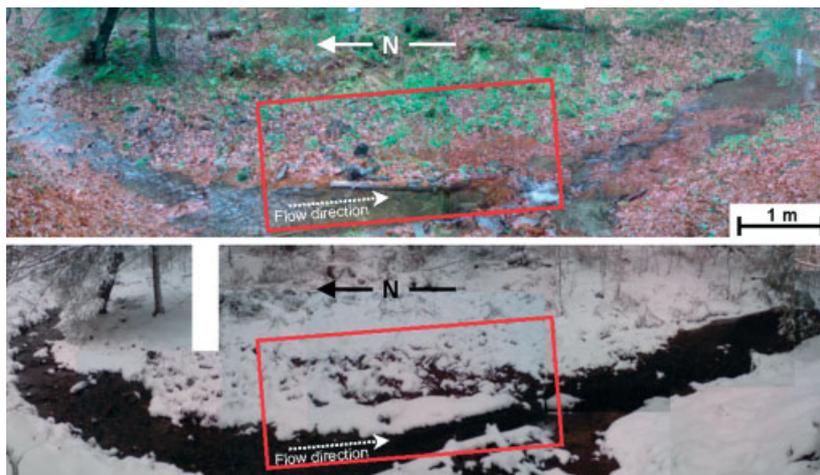
Figure 1. Investigation area in the Weierbach catchment (inside red square: approximately 5 × 3 m)—left bank riparian area
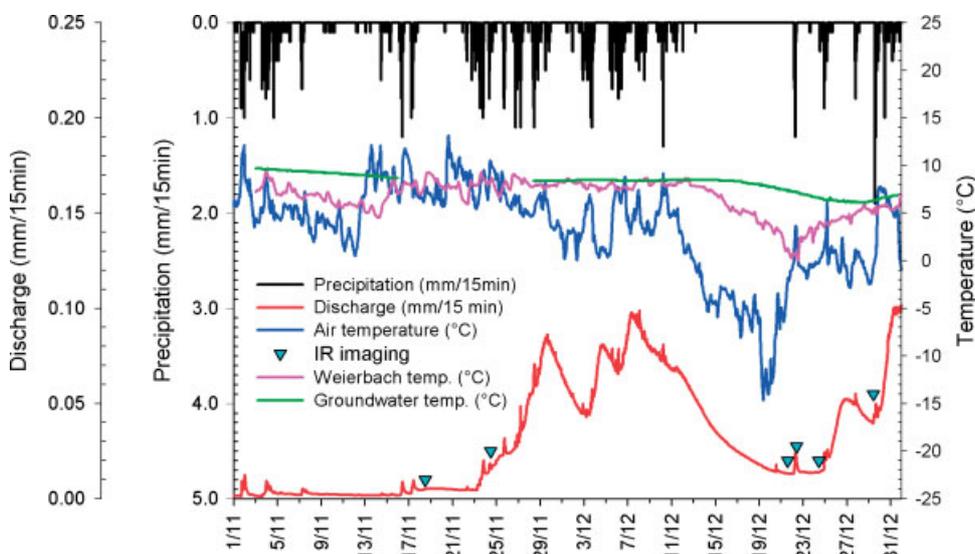
Figure 2. Weather (air temperature and rainfall), discharge, streamwater and groundwater temperature conditions at the Weierbach streamgauge station from 1 November to 31 December 2009. Thermal IR sampling points (triangles) are shown for different wetness conditions during the study period

input into the camera's computer to compensate for their effects on the temperature measurements.

Images were always taken from the same position on the right bank of the Weierbach, at an incident angle of approximately 45°. Uncertainty in incidence angle due to water surface roughness in the stream channel was considered to be small based on previous results reported by Cardenas *et al.* (2008). The thermal IR image sequence covered the gradual change in meteorological and hydrological conditions from 18 November to 29 December 2009.

Image pixels were classified as soil, hillslope outflow, channel water, surface flow, and ice/snow on the basis of probability density functions of thermal IR values. Individual patterns of surface water, consisting of either stream water, water in ponds, or soil seepage, were mapped for each thermal IR image, thus providing the dynamics of surface water flowpaths and connectivity.

Results

Meteorological conditions during our 2-month study period were dynamic with mild temperatures (monthly average 6·5 °C) and up to 150 mm of rainfall measured in November 2009. December 2009 was characterized by extremely low temperatures (down to −14·6 °C; monthly average 0·2 °C), but with dry weather during the first 2 weeks and mostly snowfall and slightly negative temperatures during the second half of the month (total monthly precipitation 109·5 mm) (Figure 2).

The Weierbach catchment produced only small amounts of run-off in response to the first events in November. Run-off ratios increased significantly after about approximately 100 mm of accumulated rainfall (beginning around 23 November 2009). Thermal infrared images cover the entire wetting-up process of the Weierbach catchment, from 18 November, prior to the onset
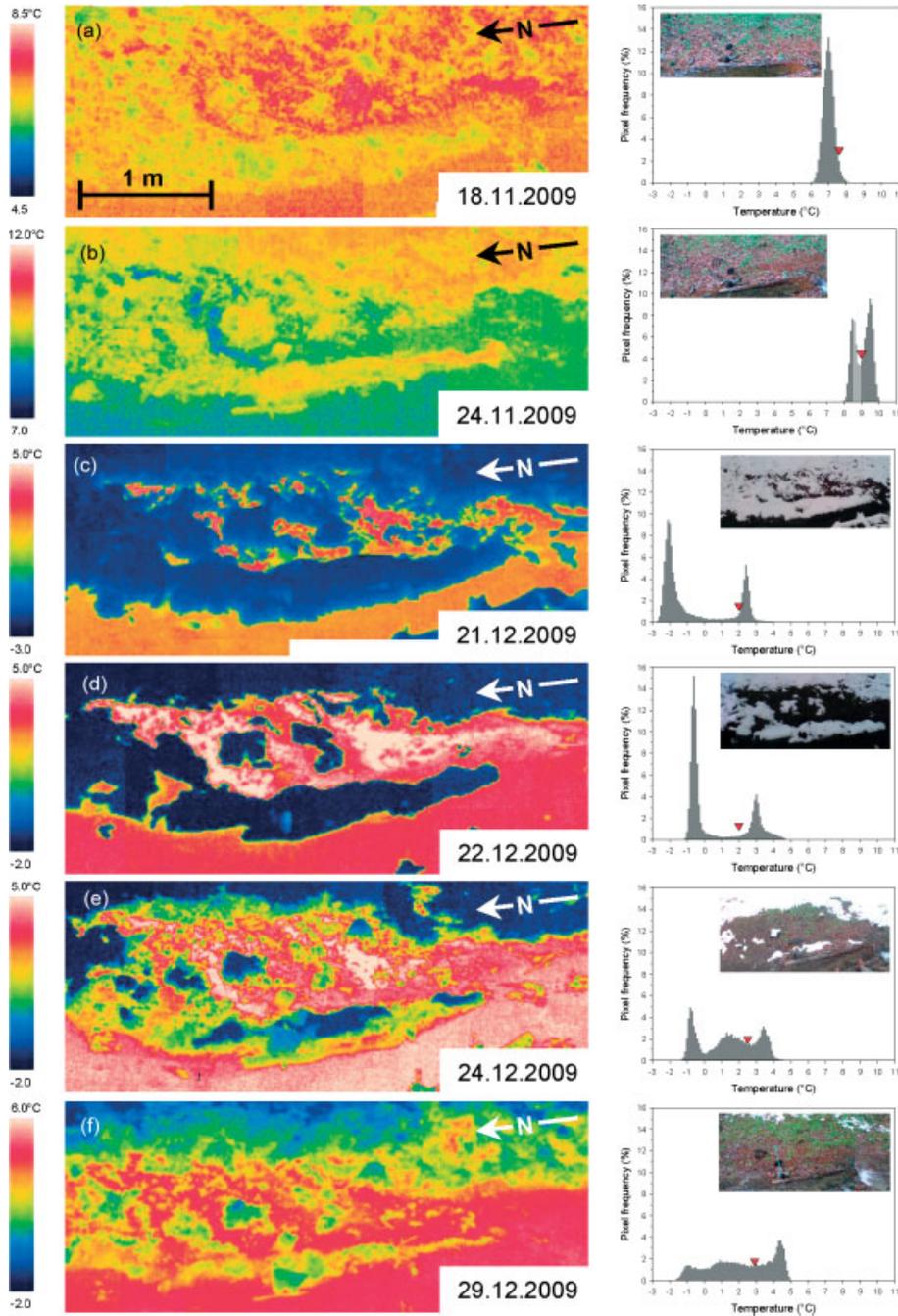
Figure 3. Thermal IR images of the left bank riparian zone in the Weierbach catchment (temperatures in°C) (left) and probability density functions of temperature pixels (right). Red triangles indicate upper [(a) 18 November 2009 (b) 24 November 2009] and lower [(c) 21 December 2009 (d) 22 December 2009 (e) 24 December 2009 (f) 29 December 2009] limits of stream temperature

of rainfall to the last image on 29 December, when more rapid surface and subsurface processes were participating in the discharge production (as shown in Figure 2).

Qualitative description of the spatial and temporal patterns of thermal infrared signatures

A initial qualitative examination of the thermal images reflected contrasting meteorological conditions between November and December 2009 (Figure 3). While the contrast between air, stream, and groundwater temperature was extremely small in November, it gradually became more pronounced throughout December with freezing conditions lasting for several weeks (Table I). On 18 November, the overall thermal IR image temperature amplitude was only 2·3 °C as a result of the air and stream temperature being almost the same (close to 7 °C). The IR probability density function of the mapped pixels was unimodal for the image taken on 18 November 2009 (Figure 3a). While the stream (orange colour), its

Table I. Air, stream and image temperature, and weather conditions during thermal IR imaging from 18 November to 29 December 2009

Date	Air temperature (°C)	Relative humidity (%)	Stream IR temperature (°C)		Image IR temp. (°C)		Weather conditions
			Minimum	Maximum	Minimum	Maximum	
18 November 2009; 12:30	7·1	89	6·8	7·5	5·9	8·2	Dry
24 November 2009; 11:30	10·5	98	8·4	8·9	7·9	10·2	Light rain
21 December 2009; 14:30	−2·2	100	2·2	2·6	−3	4·6	Snow
22 December 2009; 10:45	2·4	100	2·1	3·2	−1·2	5	Rain on snow
24 December 2009; 10:45	−0·2	100	2·5	4·2	−1·4	4·8	Dry
29 December 2009; 10:45	−0·5	100	2·9	4·7	−2	5·4	Dry

left bank, as well as parts of the riparian zone (both yellow to green colours) could be identified from the thermal IR, the warmest pixels formed patches of various sizes that were partially connected. Visual inspection of the site revealed that those areas were particularly muddy, with open water appearing locally in small ponds.

A second thermal IR image was taken on 24 November (Figure 3b), shortly after a large rainfall event (with some light rain still falling at the time of the IR image). While the air temperature was higher (10·5 °C), the overall image temperature amplitude remained small (2·3 °C). The probability density function of the imaged pixels was bimodal, suggesting a clear distinction between stream, riparian zone outflow and ponds with rain water (below 8·9 °C) and the surrounding emerging areas (above 8·9 °C).

On 21 December 2009, the study area was completely covered with snow that had fallen in the preceding days. The thermal contrast was extremely pronounced, with stream temperatures ranging between 2·2 and 2·6 °C, while the overall image temperature amplitude ranged from −3 to 4·6 °C (Table I and Figure 3c). Pixel distributions were again bimodal; snow appeared clearly in the negative temperature zone, and open water and snow-free soil were distributed through the positive temperature zone (mainly above 2·2 °C). Despite the negative ambient air temperature (−2·2 °C), quite large snow-free patches were visible inside the riparian zone. Inside these patches, temperatures locally reached up to 4·6 °C, indicating outflow of 'warm' water from the riparian soil.

With a warm front bringing thawing temperatures and rainfall, the snow cover started to melt on the 22 December 2009 (Table I and Figure 3d). The probability density function again revealed a bi-modal distribution between snow-covered and open water/emerging soil zones, but the entire distribution underwent a shift towards higher temperatures, indicating the effect of the higher air temperature and melting snow. Inside the riparian area of the image, large zones with temperatures close to that of the stream (i.e. above 2·1 °C) were identified. The thermal IR image showed clear evidence of particularly warm water emerging from the riparian zone (white pixels) and flowing towards the stream (Figure 3d).

An upstream viewing thermal IR image covering the entire area under investigation revealed the substantial temperature difference between the Weierbach and the entire left-bank riparian zone (Figure 4). While riparian soil outflows appeared to have substantially higher temperatures (white pixels) than the surroundings, the contact zone between the stream and snow cover clearly revealed thawing and mixing zones (orange to yellow colours).

The additional rainfall and snowmelt contributed to significantly increased water levels in the Weierbach stream on 24 December. Figure 3e shows an IR probability density function with three distinct modes: negative temperatures (remaining snow patches), temperatures ranging from 0 to 2·5 °C (emerging soil), and temperatures above 2·5 °C (stream water, riparian zone outflow, ponds) (Table I).

The thermal IR image taken on 29 December revealed a highly complex pattern of both isolated and connected patches within various temperature ranges (Figure 3f). With snow having largely melted and uncovered soil patches, the probability density function revealed a large proportion of pixels ranging between 0 and 2·9 °C (green to yellow colours in Figure 3). A third mode of pixels ranging between 2·9 and 5·4 °C covered both stream water and outflows in the riparian zone.

Tracing riparian water sources with thermal IR imagery

Thermal IR close-up views taken in the contact zone between the Weierbach and the riparian area on the 24 November 2009 showed an outflow of 'cold' water seeping from the right bank directly into the stream (Figure 5). With a temperature of approximately 8·2 °C, this seepage water was slightly colder than the surrounding bare soils (approximately 9·5 °C), the Weierbach (8·4–8·9 °C), and air temperature (10·5 °C). The thermal IR image showed how the seepage zone is connected to the Weierbach via a surface flowpath among litter covering the riparian soil. The image further revealed
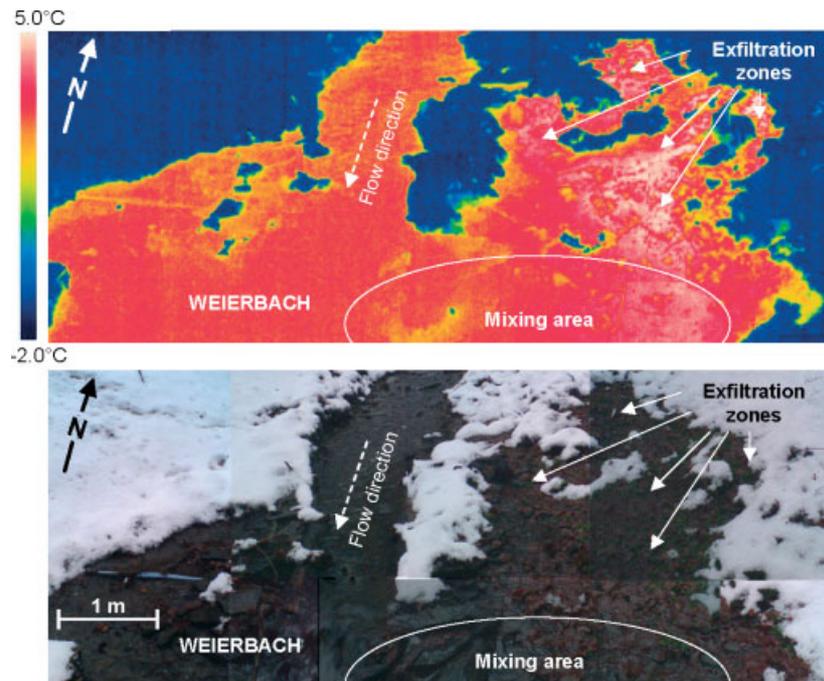
Figure 4. Up-stream thermal IR (top) and optical (bottom) view of the Weierbach (left half image) and of the left-bank snow-free riparian zone (right half image) on 22 December 2009
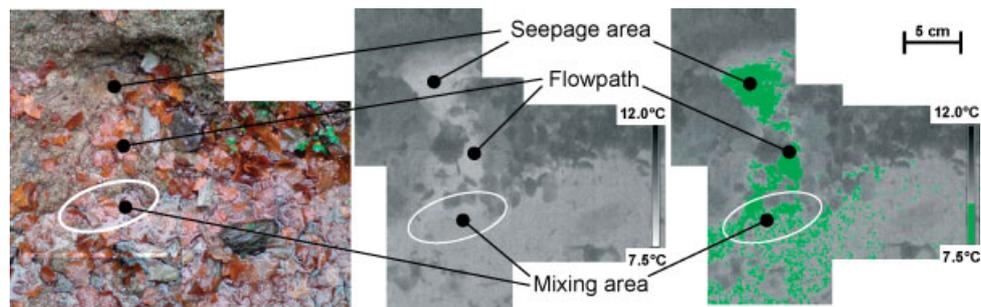
Figure 5. Right bank soil water seepage zone in the riparian area of the Weierbach close to the streamgauge on 24 November 2009 (green pixels have a temperature below 8·2 °C)

a mixing zone between the colder seepage and warmer stream water (Figure 5).

Figure 6a shows a close-up view of snowmelt in the riparian zone on the 22 December image revealing how 'warm' water (above 3 °C) emerges from two locations in the riparian soil and mixes with cold water from the melting snow cover. On the 24 December image, the saturated area became substantially larger (Figure 6b). The two 'warm' water outflow zones remained in the same locations and contributed, together with higher air temperatures and rainfall, to the progressively enlarged snow-free zone and saturated area.

Tracing surface water connectivity with thermal IR imagery

We examined the changing connectivity patterns within the six individual thermal IR images in Figure 3 by applying a temperature threshold for surface water pixel appearance. We assigned saturated and non-saturated surface water pixels to the spatial probability density functions (in Figure 3) based on a temperature threshold determined on the basis of minimum and maximum stream temperature (available from Table I):

$$\text{if} \quad \text{SIRT} > \text{EMF}: \quad \text{select pixels} \geq \text{Minimum SIRT} \quad (1)$$

$$\text{if} \quad \text{SIRT} < \text{EMF}: \quad \text{select pixels} \leq \text{Maximum SIRT} \quad (2)$$

where SIRT is the stream IR temperature and EMF are the emerging features, in this case, bare soil, litter and/or snow cover. Criterion (1) was applied for the images taken from 21 to 29 December, when stream water IR temperature systematically exceeded than that of the emerging features. When the latter were warmer than stream water, i.e. on 24 November 2009, we applied criterion (2).

Figure 7 shows the complex and changing nature of finescale HRS connectivity. These patterns reveal many
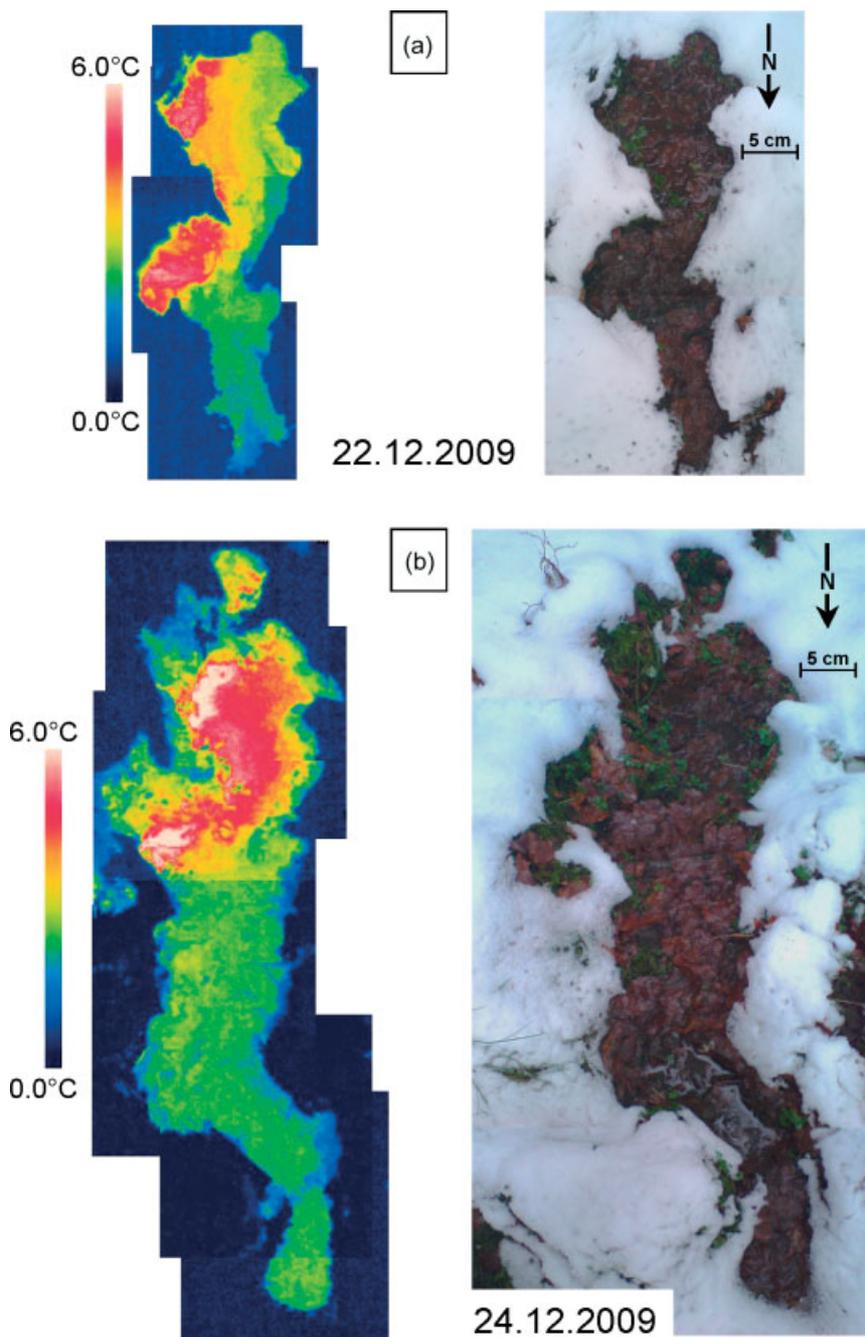
Figure 6. Thermal IR images and corresponding optical images of snow-free spots in the riparian zone of the Weierbach on (a) 22 December 2009 and (b) 24 December 2009

zones that are effectively isolated patches, disconnected from the Weierbach stream channel.

The thermal IR image taken on 18 November had a unimodal distribution, and stream IR temperature was only slightly higher than that of emerging features. Since the probability density function did not allow for a clear separation between surface water pixels and emerging soil pixels, the classification was restricted to those pixels that had a temperature that was above the maximum temperature determined for the stream surface (i.e. $7.5\,°C$). As a consequence, no pixels representing the Weierbach

itself were retained for the 18 November and only surface water patches in the riparian zone are distinguishable in Figure 7.

On 18 November, there is little connectivity between the isolated small, decimetre-scale satured patches and the stream. The time-lapse through the six events shows how dynamic this zone is, from partial connectivity on 21 December to very well-defined connectivity of all but a few patches on 22 December. Even during periods of significant connectivity, the way in which the connectedness manifests itself varies from timeperiod to timeperiod. The
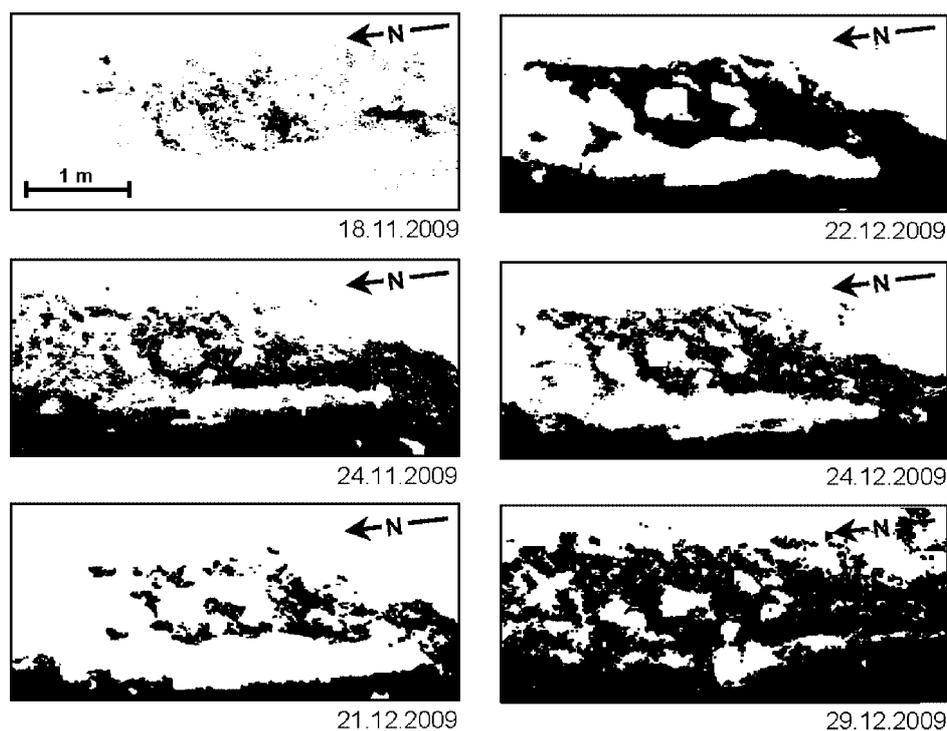
Figure 7. Time-lapse of surface water connectivity patterns in the riparian zone of the Weierbach catchment. The image covers the area delimited by the red square (5 × 3 m) depicted in Figure 1 and spans the same time periods as illustrated in Figure 3

final image on 29 December shows how isolated patches of unsatured ground can be embedded within otherwise continuous, connected, saturated zones.

Discussion and Conclusions

Our observations suggest that thermal IR imaging offers potential for locating and characterizing water contributions (e.g. soil seepage, surface run-off) from hillslopes and riparian zones to the stream channels. In particular, thermal IR offers a view into finescale processes at the HRS interface but not possible with other techniques. Such information can also eventually aid in better targeting of sampling protocols of soil water, groundwater and surface water, and building upon approaches like those in the study of McGlynn and McDonnell (2003) and Jencso *et al.* (2009) for quantifying HRS dynamics. The thermal IR images offer instantaneous surface water connectivity snap-shots, potentially covering an area ranging from a few square centimetres to several tens of square metres. As such, this technique appears to be a powerful tool to document and map how subsurface and surface filling and spilling of isolated patches of saturation lead to a generalized connectedness of larger areas, increasing both the accuracy and frequency of mapping and characterising surface saturated areas in the HRS system. In comparison to the alternative 'squishy boot' method (Dunne and Black, 1970), topography-soil-vegetation analysis (Dunne *et al.*, 1975; O'Loughlin, 1981), remote sensing (Matgen *et al.*, 2006), or GIS-based approaches (Zollweg *et al.*, 1997), simple hand-held thermal IR offers an ease of

use and level of fidelity to examine hitherto unexplored aspects of HRS behaviour.

We speculate that thermal IR imaging techniques may be complementary to conventional tracer techniques and help target water sampling protocols for the determination of geochemical, isotope, or ecological tracers. Many studies have identified the near-stream saturated zone for important partitioning of rainfall, snowmelt and exfiltrating groundwater (Sklash and Farvolden, 1979; Hooper *et al.*, 1990; Pfister *et al.*, 2009). Our example images suggest that thermal IR could be used as a tool to quantify the degree of groundwater exfiltration and hence event/pre-event mixing in turn helping to reduce uncertainties related to unstable end-member solutions (Elsenbeer *et al.*, 1995; Burns, 2002) or unrealistic mixing assumptions (McGuire and McDonnell, 2006) often encountered in tracer-based studies.

Finally, thermal IR images appear to offer some ways to quantify connectivity (Braken and Croke, 2007). In particular, our results suggest that it is possible for thermal IR imagery to allow for differentiating 'variable active' and 'variable contributing' areas and periods, as defined and advocated by Ambroise (2004). One limitation of the approach in this regard are periods of similar temperature conditions between soil water seepage, rainfall, stream water, vegetation, and air temperature. The identification of spatial patterns is rendered extremely difficult in these circumstances. As a consequence, the thermal imaging would eventually benefit from the increasingly pronounced temperature differences

as the overall temperature difference within the images becomes larger. While this technique certainly allows for investigating hydrological processes in areas that cannot be easily monitored from airborne sensor platforms (e.g. forested catchments), we expect nonetheless, the development of ground vegetation during the growing season to progressively hide thermal patterns at soil level in the riparian and/or hillslope zones. As for the interpretation of the thermal IR images, the issues and limitations raised above suggest additional investigations focusing on the development of pixel classification methodologies that rely on robust and objective selection criteria.

Despite these current shortcomings, we see great potential for linking images with chemical data for a more detailed characterization of identified patterns at the HRS interface. We are now working to mount the thermal IR camera on a platform and record images at regular intervals to monitor conditions before, during, and after rainfall events, as well as throughout seasons.

Acknowledgements

References

Ambroise B. 2004. Variable 'active' versus 'contributing' areas or periods: a necessary distinction. *Hydrological Processes* **18**: 1149–1155.

Anderson JM, Wilson SB. 1984. The physical basis of current infrared remote-sensing techniques and the interpretation of data from aerial surveys. *International Journal of Remote Sensing* **5**: 1–18.

Anderson MC, Neale CMU, Li F, Norman JM, Kustas WP, Jayanthi H, Chavez J. 2004. Up scaling ground observations of vegetation water content, canopy height, and leaf area index during SMEX02 using aircraft and Landsat imagery. *Remote Sensing of Environment* **92**: 447–464.

Cardenas BM, Harvey JW, Packman AI, Scott D. 2008. Ground-based thermography of fluvial systems at low and high discharge reveals potential complex thermal heterogeneity driven by flow variation and bioroughness. *Hydrological Processes* **22**: 980–986.

Bonell M. 1993. Progress in the understanding of runoff generation dynamics in forests. *Journal of Hydrology* **150**: 217–275.

Braken LJ, Croke J. 2007. The concept of hydrological connectivity and its contribution to understanding runoff-dominated geomorphic systems. *Hydrological Processes* **21**: 1749–1763.

Burns DA. 2002. Stormflow hydrograph separation based on isotopes: the thrill is gone—what's next?. *Hydrological Processes* **16**: 1515–1517.

Cirmo C, McDonnell JJ. 1997. Linking the hydrologic and biogeochemical controls of nitrogen transport in near-stream zones of temperate-forested catchments: a review. *Journal of Hydrology* **199**: 88–120.

Deitchman RS, Loheide SP, *II*. 2009. Ground-based thermal imaging of groundwater flow processes at the seepage face. *Geophysical Research Letters* **36**: L14401, DOI: 10.1029/2009GL038103.

Dunne T, Black RD. 1970. Partial area contributions to storm runoff in a small New England watershed. *Water Resources Research* **6**: 1296–1311.

Dunne T, Moore TR, Taylor CH. 1975. Recognition and prediction of runoff-producing zones in humid regions. *Hydrological Sciences Bulletin* **20**: 305–327.

Elsenbeer H, Lorieri D, Bonell M. 1995. Mixing model approaches to estimate storm flow sources in an overland flow-dominated tropical rainforest catchment. *Water Resources Research* **31**: 2267–2278.

Frankenberger JR, Brooks ES, Walter MT, Walter MF, Steenhuis TS. 1999. A GIS-based variable source area hydrology model. *Hydrological Processes* **13**: 804–822.

Gburek WJ, Drungil CC, Srivivasan MS, Needelman BA, Woodward DE. 2002. Variable-source area controls on phosphorus transport: Bridging the gap between research and design. *Journal of Soil Water and Conservation* **57**: 534–543.

Gu R, Montgomery S, Al Austin T. 1998. Quantifying the effects of stream discharge on summer river temperature. *Hydrological Sciences Journal* **43**: 885–904.

Hooper RP, Christophersen N, Peters NE. 1990. Modeling streamwater chemistry as a mixture of soil water end-members—an application to the Panola Mountain catchment, Georgia, USA. *Journal of Hydrology* **116**: 321–343.

Jencso KG, McGlynn BL, Gooseff MN, Wondzell SM, Bencala KE, Marshall LA. 2009. Hydrologic connectivity between landscapes and streams: Transferring reach- and plot-scale understanding to the catchment scale. *Water Resources Research* **45**: W04428, DOI:10.1029/2008WR007225.

Kies A, Hofmann H, Tosheva Z, Hoffmann L, Pfister L. 2005. Using 222Rn for hydrograph separation in a micro basin (Luxembourg). *Annals of Geophysics* **48**: 101–107.

Krein A, Salvia-Castellvi M, Iffly JF, Barnich F, Matgen P, Van den Bos R, Hoffmann L, Hofmann H, Kies A, Pfister L. 2007. Uncertainty in chemical hydrograph separation. In *Proceedings of the 11th ERB conference. Uncertainties in the 'monitoring-conceptualisation-modelling' sequence of catchment research*. Pfister L, Hoffmann L (eds). IHP-VI Technical Documents in Hydrology 81: Luxembourg; 20–22 September 2006. 21–26.

Kuo WL, Steenuis TS, McCulloch CE, Mohler CL, Weinstein DA, DeGloria SD, Swaney DP. 1999. Effect of grid size on runoff and soil moisture for a variable-source-area hydrology model. *Water Resources Research* **35**: 3419–3428.

Martínez-Carreras N, Krein A, Iffly JF, Barnich F, Pfister L, Hoffmann L, Gallart F. 2010. *Examining the spatial and temporal variations of erosion processes and hydrochemical response in mesoscale catchments—preliminary results from the Attert basin in Luxembourg*. Mitteilungen aus der Forschungsanstalt für Waldökologie und Forstwirtschaft (FAWF) Rheinland-Pfalz 64: 125–134.

Matgen P, Henry JB, Hoffmann L, Pfister L. 2006. Assimilation of remotely sensed soil saturation levels in conceptual rainfall-runoff models. In *Prediction in ungauged basins: promise and progress*, Sivapalan M, Wagener T, Uhlenbrook S, Zehe E, Lakshmi V, Liang X, Tachikawa Y, Kumar P(eds).,). IAHS Publication 303: 226–234.

McGlynn BL, McDonnell JJ. 2003. Quantifying the relative contributions of riparian and hillslope zones to catchment runoff. *Water Resources Research* **39**: 1310, DOI:10.1029/2003WR002091.

McGuire KJ, McDonnell JJ. 2006. A review and evaluation of catchment transit time modeling. *Journal of Hydrology* **330**: 543–563.

Ogden FL, Watts BA. 2000. Saturated area formation on nonconvergent hillslope topography with shallow soils: a numerical investigation. *Water Resources Research* **36**: 1795–1804.

O'Loughlin EM. 1981. Saturation regions in catchments and their relations to soil and topographic properties. *Journal of Hydrology* **53**: 229–246.

3131

Pfister L, McDonnell JJ, Wrede S, Hlúbiková D, Matgen P, Fenicia F, Ector L, Hoffmann L. 2009. The rivers are alive: on the potential for diatoms as a tracer of water source and hydrological connectivity. *Hydrological Processes* **23**: 2841–2845.

Roth TR, Westhoff MC, Huwald H, Huff JA, Rubin JF, Barrenetxea G, Vetterli M, Parriaux A, Selker JS, Parlange MB. 2010. Stream temperature response to three riparian vegetation scenarios by use of a distributed temperature validated model. *Environmental Science and Technology* **44**: 2072–2078, DOI: 10.1021/es902654f.

Roxburgh IS. 1985. Thermal infrared detection of submarine springs associated with the Plymouth Limestone. *Hydrological Sciences Journal* **30**: 185–196.

Selker JS, Thévenaz L, Huwald H, Mallet A, Luxemburg W, van de Giesen N, Stejskal M, Zeman J, Westhoff M, Parlange MB. 2006. Distributed fiber-optic temperature sensing for hydrologic systems. *Water Resources Research* **42**: W12202, DOI:10.1029/2006WR005326.

Sklash MG, Farvolden RN. 1979. Role of groundwater in storm runoff. *Journal of Hydrology* **43**: 45–65.

Smith K. 1981. The prediction of river water temperatures. *Hydrological Sciences Bulletin* **26**: 19–32.

Verhoest NEC, Troch PA, Paniconi C, De Troch FP. 1998. Mapping basin scale variable source areas from multitemporal remotely sensed observations of soil moisture behavior. *Water Resources Research* **34**: 3235–3244, DOI:10.1029/98WR02046.

Webb BW, Nobilis F. 1995. Long term water temperature trends in Austrian rivers. *Hydrological Sciences Journal* **40**: 83–96.

Webb BW, Walling DE. 1985. Temporal variation of river water temperatures in a Devon river system. *Hydrological Sciences Journal* **30**: 449–464.

Webb BW, Walling DE. 1992. Long term water temperature behaviour and trends in a Devon, UK, river system. *Hydrological Sciences Journal* **37**: 567–580.

Zollweg JA, Gburek WJ, Pionke HB, Sharpley AW. 1997. GIS-based delineation of source areas of phosphorus within agricultural watersheds of the northeastern USA. In *Modelling and Management of Sustainable Basin-Scale Water Resource Systems*, Simonovic SP, Kundzewicz Z, Rosbjerg D, Takeuchi K(eds).,). IAHS Publication 231: 31–39.